Modulation of the Photophysical Properties of C_{60} by Electronic Confinement Effect

F. Márquez*,† and M. J. Sabater‡

School of Science and Technology, University of Turabo, P.O. Box 3030, Gurabo, Puerto Rico 00778-3030, and Instituto de Tecnologia Quimica, Universidad Politecnica de Valencia, CSIC, 1-Avenido Naranjos S/N, 46071 Valencia, Spain

Received: October 16, 2004; In Final Form: December 10, 2004

This research work reports on the incorporation of fullerene C_{60} in diverse inorganic and organic matrixes and how these different environments induce changes on the photophysical properties of the molecule depending on the cavity dimensions of the host. Indeed the fluorescence emission band of C_{60} experiences a progressive bathochromic shift with respect to C_{60} in solution as the cavity dimensions of the host decrease in going from the mesoporous material MCM41 to UTD-1 and Na−Y zeolites. This experimental observation, which has been documentarily confirmed by theoretical predictions and recent experimental results, is a reflection of the confinement effect imposed by the host. However, the most striking result reported in this work is that the fluorescence range accessible to this occluded species can be extraordinarily extended by confinement inside the neutral cages of a "dendritic box". The ability of the dendritic shell to create a microenvironment, modifying the properties of its functional core, allows the emission bands of C_{60} incorporated into a dendrimer to be effectively red-shifted with respect to their emission in solution, and, contrarily to other confined spaces of considerable hardness such as zeolites or the high surface material MCM41, the magnitude of this shifting is maximum and can be modulated under appropriate experimental conditions. This phenomenon has an enormous relevance since it can be exploited in future technological applications.

1. Introduction

The unique physical and chemical properties of fullerene C_{60} have drawn much attention in the past few years for designing devices able to perform complex functions such as molecular switches, receptors, photoconductors, photoactive dyads, and sensors, etc.[1−3] Indeed, to gain control over the superconducting, optical, and other molecular properties of buckminsterfullerene, C_{60}, an intensive effort is being devoted to developing supramolecular systems where intermolecular interactions can be avoided.[2−8] A general methodology to obtain isolated molecules consists of the confinement of a guest within solid matrixes such as zeolites or alternatively by forming inclusion complexes within cyclodextrin and calixarenes in aqueous solutions.[9−15] Indeed, it is well-known that the interaction experienced by a guest molecule with a zeolite that is acting as a host is drastically different from the interaction with solvent molecules, hence explaining the long list of reports devoted to the incorporation of organic guests into these rigid aluminosilicates. For this reason and taking into account that C_{60} is a spherical molecule of 7.9 Å crystallographic diameter, previous studies have been aimed at incorporating fullerenes in extralarge-pore aluminophosphates such as ALPO-5, VPI-5 (pore diameter, 12.1 Å), and ALPO-8 (pore diameter, 7.9 × 8.7 Å) serving as confined microreactors.[9−13] In addition these studies have been extended to the occlusion of C_{60} molecules in mesoporous MCM41 type solids as their pore diameter can be accurately tuned, ranging from 2 to 25 nm.[16]

In close connection with this topic, it is necessary to point out that the incorporation of laser dye molecules within the internal cavities of a macromolecular dendritic structure has also been described recently.[17] Effectively, several dyes have been entrapped into the so-called "dendritic box", a sort of cavity formed within a fifth generation poly(propyleneimine) dendrimer with terminal bulky substituents, typically N-t-BOC-protected phenylalanine. These terminal N-t-BOC-protected amino acids are able to "hermetically" lock the internal space of the macromolecule, therefore preventing the flux of matter through the dendrimer.[17] On this basis, a variety of guest molecules have been physically trapped within these internal voids by constructing the dense shell in their presence. This has served to show that the photophysical properties of the guests encapsulated into the dendritic box can be easily modulated by electron confinement effect (an electron effect that is stronger as the size of the confined guest approaches the cavity dimensions of the host and manifests itself in a gradual bathochromic shift of the fluorescence emission of the entrapped molecule).[18]

In this piece of research we report a study on the confinement of C_{60} fullerene in different inorganic matrixes of decreasing pore size such as UTD-1 and Na−Y zeolites and the mesoporous material MCM41. The work reports on the progressive bathochromic shift of the fluorescence emission of C_{60} as the cavity size of the inorganic host decreases and more importantly that this fluorescence emission can be extraordinarily extended by confinement inside the neutral cages of a dendrimer. Effectively, in this case and unlike the former inorganic hosts of considerable hardness, the magnitude of this shifting is utmost and can be modulated under appropriate experimental conditions. This peculiar effect could have unprecedented applications in the development of supramolecular devices related to the tuning of photophysical properties of confined molecules.[18]

* Corresponding author. E-mail: fmarquez@suagm.edu.
† University of Turabo.
‡ Universidad Politecnica de Valencia.

10.1021/jp045263k CCC: $30.25
Published on Web 02/04/2005

2. Experimental Section

2.1. Host Materials. Na−Y zeolite (having spherical supercages of 1.3 nm diameter tetrahedrally interconnected through 0.74 nm windows; Si/Al, 2.5; average crystal size, 0.4−0.6 μm) was a commercial sample supplied by PQ Corp.[19,20]

UTD-1 zeolite (Si/Al, ∞) is the largest pore zeolite known with channels defined by 14 Si atoms and dimensions of 1.0 × 0.75 nm. It was prepared according to the synthesis method described previously in the literature.[21]

MCM41 (Si/Al, ∞), a material described in terms of a preferred honeycomb-like structure with a pore diameter of 3.5 nm and a wall thickness of ca. 1.1 nm, was prepared according to a recently reported procedure.[22]

The dendrimer was built up from a commercial sample of a fifth generation poly(propyleneimine) dendrimer with 64 terminal amine groups supplied by Aldrich.

2.2. Incorporation of C_{60} in the Hosts. Adsorptions of C_{60} were carried out by heating a mechanical mixture of C_{60} (40 mg) and zeolite (Na−Y or UTD-1) or the mesoporous material MCM41 (500 mg) in an oven at 400 °C under reduced pressure (1 Torr) for 1 month in the case of zeolites and for 6 h in the case of the material MCM41. The samples were thoroughly extracted in micro-Soxhlet equipment using CH_2Cl_2 as solvent.

Incorporation of C_{60} in the fifth generation dendrimer was carried out by adding 50 mg of commercial C_{60} to a solution of 50 mg of dendrimer DAB-dend-(NH-*t*-BOC-L-Phe)$_{64}$ (64 end amine groups) in 5 mL of CH_2Cl_2 with 1 mL of triethylamine, and the solution was stirred for 24 h at room temperature. Then 161 mg of N-tBOC-L-phenylalanine *N*-hydroxysuccinimide ester was added, and the solution was stirred overnight. Dilution to 50 mL with dichloromethane was followed by washing with water and saturated Na_2CO_3 solution. The organic layer was dried with $MgSO_4$, and the solvent was evaporated under vacuum to afford the C_{60}-doped dendrimer. The C_{60}-doped dendrimer was purified by dialysis until no traces of free C_{60} were detected by HPLC.

2.3. Characterization. The purity and crystallinity of the inorganic solids were determined by X-ray diffraction (XRD) using a Siemens D500 instrument (Cu Kα radiation and graphite monochromator), provided with a variable divergence slit and working in the fixed irradiated area mode. The crystallinity of the zeolites was calculated from the intensity of the 22^o 2θ peak in reference to the corresponding standard sample (it has to take into account that after loading with C_{60} the crystallinity of the zeolitic materials was almost unaltered). Combustion chemical analyses were performed in a Perkin-Elmer analyzer. Thermogravimetry−differential scanning calorimetry tests were carried out under an air stream on a Netzch STA-409 thermobalance using kaolin as standard.

FT-Raman spectra were recorded on a Bruker spectrometer, model RFS 100/s. The 1064 nm line of a diode pumped Nd:YAG laser was used for excitation along with a high-sensitivity germanium diode detector, cooled to liquid nitrogen temperature. The laser Raman spectra were examined in the 180° scattering configuration using a sample cup specially designed for this study. About 10 mg of each sample was pressed into the sample cup and then mounted on the sample holder. Various laser powers were tried so that the optimum power (130 mW) was selected. The sample temperature was controlled by measuring the Stokes/anti-Stokes intensity ratio of Raman scattered radiation. The spectral resolution and reproducibility was experimentally determined to be better than 4 cm^{-1}, and the number of scans varied from 700 to 3000 with recording times of 30 min to 2 h. The Raman spectra were corrected for instrumental response using a white light reference spectrum.

The XP spectra were obtained with a VG-Escalab 210 electron spectrometer, by using a nonmonochromatic Al Kα (1486.7 eV) source of a twin anode in the constant analyzer energy mode with a pass energy of 40 eV. To remove charging shifts and deal with Fermi edge coupling problems, binding energies were scaled against the peak of the Si 2p of the silicoaluminate framework. The pressure of the analysis chamber was maintained at 5 × 10^{-10} mB.

In the case of inorganic hosts, direct evidence of the external versus internal location of C due to the incorporation of fullerene has been obtained by carrying out XPS analysis of the exposed external surface of the particle. Herein, we have combined this technique with progressive sputtering with a fast Ar^+ beam that produces increasing decapping of the external layers of the particles. In this way it is possible to map out the C level from the exterior to the interior of the solid particle up to a depth of several hundred angstroms.

For cryo-SEM (SEM = scanning electron microscopy) measurements samples were transferred to the preparation chamber of an OXFORD CT-1500 Cryotrans System and cooled to −170 °C. Next samples were placed on the precooled stage of a Zeiss DSM 960 scanning electron microscope and were partially etched with an electron beam to partially remove the surface solvent.

3. Results

Fullerene C_{60} has been incorporated within different inorganic hosts of increasing pore size such as zeolite Na−Y (0.72 nm), extralarge-pore zeolite UTD-1 (1.0 × 0.75 nm), and the mesoporous material MCM41 (3.5 nm) through vapor-phase adsorptions of C_{60} under reduced pressure (1 Torr) at 400 °C (see Experimental Section).

Direct evidence of the internal location of C_{60} within these siliceous materials has been obtained by carrying out XPS analysis of the C-to-Si atomic ratio of the exposed external surface of the particle. Thus, by combining this technique with a progressive sputtering with a fast Ar^+ beam that produces increasing decapping of the external layers of the inorganic solids, it is possible to map out the C-to-Si atomic ratio from the exterior to the interior of the solid particle up to a depth of several hundred angstroms.

The results obtained for sample C_{60}@Na−Y are shown in Figure 1. Each point corresponds to the average of five independent measurements, and the area corresponding to the peaks due to C and Si was calibrated to account for the different response of C and Si atoms. From these data it can be clearly stated that carbon atoms are spread out through the whole particle. The last experimental points were obtained at ca. 20 nm depth, corresponding to more than 10 supercages depth from the external surface of the particles. The mean C-to-Si atomic ratio of the whole particle calculated from the TG analysis was ca. 0.1. This value is indicated by dots in Figure 1. From these experimental results it is clear that the TG value is a weighted average of different populations. Thus, while the C-to-Si atomic ratio of the external surface is lower than the average, the carbon content progressively increases as we penetrate into the particle, reaching a plateau of 0.26 at ca. 20 nm from the external surface.

Additional evidence for the incorporation of C_{60} into this inorganic host was also obtained by nitrogen adsorption−desorption BET surface area measurements. Indeed, the data revealed a significant reduction of the pore volume of the zeolite

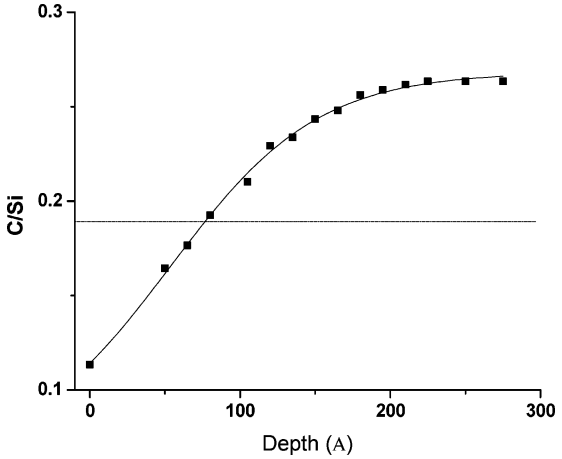

Figure 1. Plot of the C-to-Si atomic ratio measured by XPS analysis of C_{60}@Na−Y vs the depth of the particle. Each point is the average of five independent measurements. Sputtering has been achieved by using an Ar^+ beam. The horizontal line corresponds to the average C-to-Si atomic ratio obtained from thermogravimetric analysis.

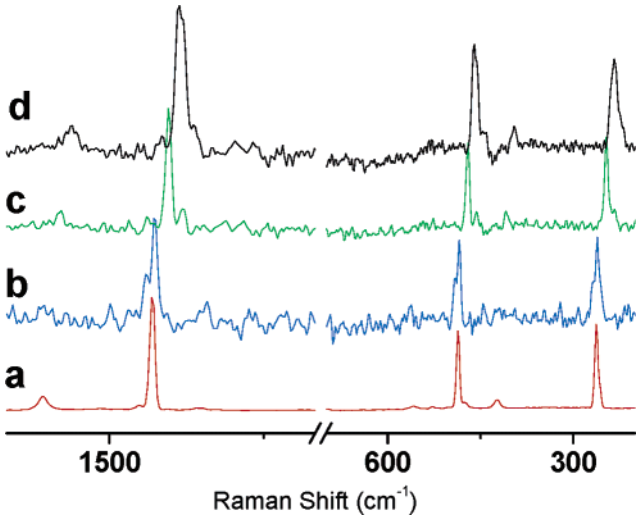

Figure 2. Near-IR−FT-Raman spectra of neat fullerene C_{60} (a), C_{60}@MCM41 (b), C_{60}@UTD-1 (c), and C_{60}@Na−Y (d), showing the vibrations attributed to the stretching modes of fullerene C_{60}.

from 0.31 to 0.06 $cm^3\ g^{-1}$ after inclusion of fullerene C_{60} (a fact that supports the pore filling with C_{60} entities).

The loaded materials were characterized by FT-Raman spectroscopy. Thus, as can be followed from Figure 2a, the Raman spectrum of a pure sample of homogeneous C_{60} [23] has three characteristic bands at 1466, 495, and 271 cm^{-1} that have been associated with vibrational modes A_{g2}, A_{g1}, and H_{g1}, respectively, whereas the Raman spectra of fullerene incorporated in Na−Y and UTD-1 zeolites as well as in the mesoporous material MCM-41 exhibit similar bands, although slightly red-shifted. This shift could possibly be the result of geometrical distortions of the molecule imposed by the inorganic hosts (Figure 2). In this respect, it is necessary to point out that despite immobilization of C_{60} into the cages or channels of the zeolites being surely more appealing than incorporation into mesoporous material MCM-41 due to the nonexistence of hindrances or physical barriers in the latter pores, the rigid walls of MCM-41 are still able to produce an appreciable interaction with the molecular structure of C_{60} in view of the slight shifting of the vibration bands upon adsorption on this material.

On the other hand, the loaded inorganic matrixes were also characterized by diffuse reflectance spectroscopy (see Figure 3). Indeed, fullerene C_{60} absorbs in the UV region, showing two maxima at ca. 260 and 330 nm and a very weak band ranging from 430 to 640 nm in cyclohexane solution. The UV−vis spectra of the loaded solids displayed similar bands, although blue-shifted with respect to neat C_{60} solution or C_{60} solid (see Figure 3a and the insert corresponding to the absorption spectrum of C_{60} in cyclohexane solution at room temperature). In fact, the intensity of the broad band observed in solution in the range of 430 to 640 nm was importantly increased under incorporation into the inorganic matrixes. The constraints exerted by the inorganic hosts on fullerene C_{60} could lead to symmetry breaking and correlative to the occurrence of transitions which are forbidden in the case of isolated C_{60} molecules or also to the increase of the molar absorptivities.[24]

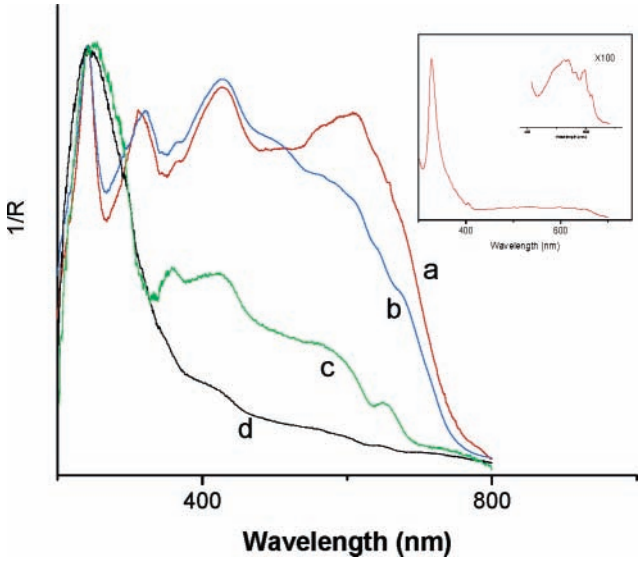

Figure 3. Diffuse reflectance spectra (1/*R*) of fullerene C_{60} bulk (a), C_{60}@MCM41 (b), C_{60}@UTD-1 (c), and C_{60}@Na−Y (d). The insert corresponds to the UV−visible absorption spectrum of C_{60} in cyclohexane at room temperature showing the extended visible range.

In the hope that the confinement effect of C_{60} into the hosts would give interesting properties to the trapped molecule, the emission spectra of C_{60} included in these inorganic materials were recorded under identical experimental conditions. In this regard it is interesting to notice that the transition between the lowest unoccupied molecular orbital LUMO and the highest occupied molecular orbital HOMO of C_{60} molecule is optically forbidden; thus, the corresponding fluorescence intensity associated with the singlet excited state is usually so weak that it can only be successfully observed at low temperature.[25−27] However, in this research work an appreciable fluorescence band was measured for C_{60} molecules confined in Na−Y and UTD-1 zeolites as well as in the high surface material MCM41 at room temperature. This experimental observation is in agreement with the enhanced fluorescence reported in previous studies of C_{60} immobilized in cages or pores of diverse zeolites.[28] Indeed, Figure 4 shows the strong fluorescence response of these C_{60}-doped materials after excitation at 428 nm at room temperature. This fluorescence emission is characterized by the presence of vibrational structure, showing three overlayed peaks. Similar fluorescence response was obtained under excitation at 320 and 250 nm.

Besides this highlighted result, the emission band in the fluorescence spectra experienced a progressive bathochromic shift with respect to C_{60} bulk at 77 K (Figure 4a) as the cavity dimensions of the inorganic host decreased from MCM41 to UTD-1 and Na−Y (see Figure 4). This spectral shift in the

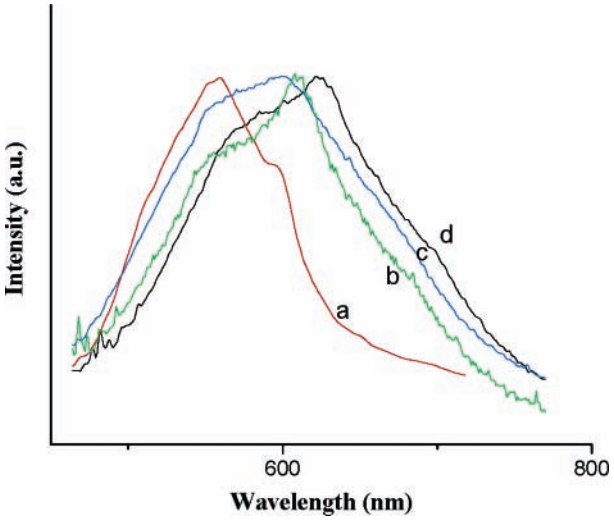

Figure 4. Normalized emission spectra of (a) C_{60} bulk measured at 77 K and (b) C_{60}@MCM41, (c) C_{60}@UTD-1, and (d) C_{60}@Na−Y measured at room temperature, all of them after 428 nm excitation. In the case of C_{60} confined into the hosts, similar results were obtained after excitation at 320 and 250 nm.

fluorescence band has been attributed to the orbital confinement effect of organic guests when these are included in a host and is based on the concept that the molecular orbitals of the adsorbate inside the host cavity are not extended over the whole space, as they are in the gas phase, but instead are forced to limit within a reduced space.[23] This confinement effect, which is stronger as the size of the confined guest approaches the cavity dimensions, produces an energy increase of all molecular orbitals, the HOMO being more sensitive than the LUMO. Hence, the resulting effect is a reduction of the HOMO−LUMO energy gap that is reflected in the optical properties of the guest, particularly the bathochromic shift of the fluorescence emission.[29] In principle, this confinement effect can be used to modify the fluorescence emission of many interesting organic species toward less energetic wavelengths to an extent that will depend on the dimensions of the cavity hosts. The hosts should thus be chosen as a function of the magnitude of shifting needed or required in each particular case.

On the other hand, we have recently shown that the use of a particular dendrimer as organic host can be taken as a more advantageous alternative to the use of rigid inorganic matrixes since the degree of confinement in the internal cavities of a dendrimer can be efficiently regulated under appropriate experimental conditions.[18] Effectively, Meijer and co-workers reported that the modification of terminal amine functionalities of DAB-dend-$(NH_2)_{64}$ with bulky substituents, typically N-t-BOC-protected phenylalanine, results in the formation of a structure with a solid shell and a flexible core, the so-called dendritic box (DAB-dend-(NH-t-BOC-L-Phe)$_{64}$). Within the internal cavities of this macromolecular structure it is possible to encapsulate guest molecules provided the dense external shell formed with the N-t-BOC-protected amino acid is able to hermetically lock the internal space, therefore preventing the flux of matter through the dendrimer.[17] Hence, a variety of guest molecules can be physically trapped within these macroscopic vessels by constructing the dense shell in their presence. For the investigation presented here, C_{60} was encapsulated into a dendritic box constructed from a fifth generation poly(propileneimine) dendrimer with 64 terminal amine groups (DAB-dend-(NH-t-BOC-L-Phe)$_{64}$) and an L-phenylalanine derivative (see Experimental Section). This nanocomposite was characterized by matrix-assisted laser desorption ionization time-of-flight mass spectroscopy (MALDI-TOF-MS) and the concentration of C_{60} was estimated by UV−vis spectroscopy. In this regard, the loading level of the fullerene incorporated into the dendritic structure was ca. 4 molecules per dendrimer. Hence, once the C_{60}-doped dendrimer was conveniently characterized its emission spectrum was recorded in *n*-pentane at room temperature (see Figure 5). The fluorescence spectrum revealed that the confinement into a dendritic structure had a noticeable influence on the emission spectra of the guest molecule since under these conditions the emission band of C_{60} experienced a strong bathochromic shift of ca. 132 nm with respect to the emission of C_{60} in solution (λem = 675 nm after λ = 285 nm excitation). This impressive red shifting, which is undoubtedly stronger than what is measured when fullerene is confined within the rigid walls of a zeolite or the mesoporous material MCM-41, can be additionally modulated by solvent effect (see Table 1). Solvents of polarity different from that of the dendrimer can indeed induce a remarkable decreasing of the initial total volume of the macromolecular host structure due to strong repulsions between this nanocomposite and the solvent. This effect can cause an important reduction of the original size of the macromolecule, making the internal cavities of the dendrimer become smaller, hence producing effective interactions with the electronic orbitals of the guest.

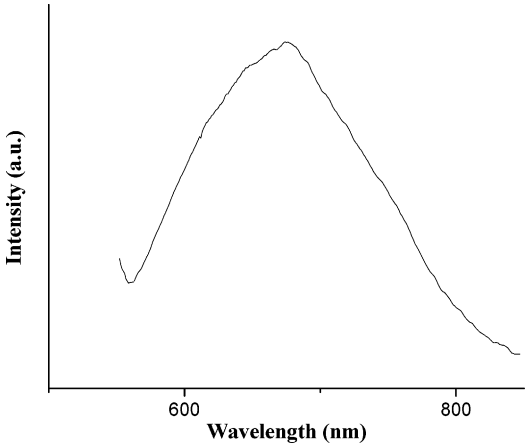

Figure 5. Emission spectrum of C_{60}@dendrimer in methanol solution at room temperature after 285 nm excitation.

TABLE 1: Fluorescence Emission Data, Obtained at Room Temperature, of C_{60}@dendrimer in Solution (after λ = 285 nm Excitation)

solvent	fluorescence	solvent	fluorescence
ethanol	625	dichloromethane	651
methanol	631	*n*-pentane	675[a]

[a] The fluorescence intensity was substantially decreased with respect to polar solvents.

Experimental evidence of this dynamic equilibrium observed in dendrimers exposed to different polarity environments has been obtained from cryo-SEM. Cryo-SEM was the method of choice for investigating the dendritic structures in different solvents because the samples were in solution. This technique can be a particularly useful method for studying new types and interaction modes among solvents and dendrimers. This study was performed on the neat dendrimer in ethanol and *n*-hexane. Samples were cooled to −170 °C and subsequently analyzed. Figure 6 shows the results obtained by cryo-SEM, indicating that increasing the polarity (in going from *n*-hexane to ethanol) substantially modifies the molecular aggregation state of the doped dendrimers.

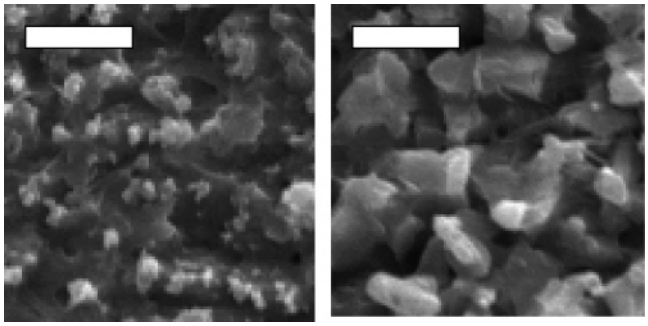

Figure 6. Cryo-scanning electron microscopy of C_{60}@dendrimer in ethanol (a) and *n*-pentane (b). From this figure can be derived the different aggregation states depending on the solvent polarity. Bar = 100 nm.

As a result, there will be changes in the energy levels of the guest to an extent that will depend on the degree of interaction with the branches of the macromolecule. Obviously, this effect should be maximized when a tight fit between the host cavity and the guest occurs, a condition that the relatively flexible walls of a dendrimer fulfill apparently to a large extent under these experimental conditions. This experimental observation has very important repercussions insofar as the emission properties of an organic guest can be modulated throughout a very broad interval in the UV−vis spectral range (impressively higher than when the guest is confined into rigid inorganic matrixes). This property, which can be appropriately modulated by accurately adjusting the medium polarity, makes supramolecular fullerene an attractive component to be incorporated in functional molecular assemblies and supramolecular arrays.

4. Conclusions

In this work we report that the fluorescence emission of bukminsterfullerene molecules can be strongly red-shifted with respect to the fluorescence emission in solution by incorporation into microporous hosts such as Na−Y and UTD-1 zeolites as well as in the mesoporous material MCM41. The magnitude of this shifting is more pronounced when the cavity size and the molecule dimensions are closer.

Contrarily to these confined spaces of considerable hardness, the magnitude of this shifting can be modulated upon incorporation into a dendrimer under appropriate experimental conditions. Effectively, despite the soft walls offered by the confined space of a dendrimer, the relative flexibility of this hyperbranched structure can get a much closer host−guest fit than the one previously measured for inorganic hosts. This is reflected in the dramatic changes observed in the spectral properties of fullerene incorporated into a dendrimer by changing the solvent polarity. This result can be justified as due to the presence of unexpectedly larger electronic constraints coming from closer host−guest tight fit. These results may have relevant implications from a technological point of view since the loaded dendrimer would help to modify the properties of the guest by simply choosing a solvent of adequate polarity or even a mixture of solvents to obtain the polarity index appropriate.

Acknowledgment. Generous financial support by the Comision Interministerial de Ciencia y Tecnologia (CICYT) of Spain (Project MAT2002-04421-C02-01) and from NASA (Grant NAG10-335) is gratefully acknowledged.

References and Notes

(1) Balch, A. L.; Olmstead, M. M. *Chem. Rev.* **1998**, *98*, 2123.
(2) Diederich, F.; Gómez-López, M. *Chem. Soc. Rev.* **1999**, *28*, 263.
(3) Wudl, F. *J. Mater. Chem.* **2002**, *12*, 1959.
(4) Latassa, D.; Enger, O.; Thilgen, C.; Habicher, T.; Offermanns, H.; Diederich, F. *J. Mater. Chem.* **2002**, *12*, 1993.
(5) Zhu, L.; Li, Y.; Wan, J.; Shen, J. *J. Appl. Phys.* **1995**, *77*, 2801.
(6) Amao, Y.; Okura, I. *Analusis* **2000**, *28*, 847.
(7) Brusatin, G.; Signorini, R. *J. Mater. Chem.* **2002**, *12*, 1964.
(8) Zhu, L.; Li, Y.; Wang, J.; Shen, J. *Chem. Phys. Lett.* **1995**, *239*, 393.
(9) Gu, G.; Ding, W.; Cheng, G.; Zhang, S.; Du, Y.; Yang, S. *Chem. Phys. Lett.* **1997**, *270*, 135.
(10) Kwon, O. H.; Yoo, H.; Park, K.; Tu, B.; Ryoo, R.; Jang, D. J. *J. Phys. Chem. B* **2001**, *105*, 4195.
(11) Kwon, O. H.; Park, K.; Tu, B.; Jang, D. J. *Chem. Phys. Lett.* **2001**, *346*, 195.
(12) Lamrabte, A.; Janot, J. M.; Elmidaoui, A.; Seta, P.; Menorval, L. C.; Backov, R.; Roziere, J.; Sauvajol, J. L.; Allègre, J. *Chem. Phys. Lett.* **1998**, *295*, 257.
(13) (a) Gügel, A.; Müllen, K.; Reichert, H.; Schmidt, W.; Schön, G.; Schüth, F.; Spikermann, J.; Titman, J.; Unger, K. *Angew. Chem., Int. Ed. Engl.* **1993**, *32*, 556, and references therein. (b) Anderson, M. W.; Shi, J.; Leigh, D. A.; Moody, A. E.; Wade, F. A.; Hamilton, B.; Carr, S. W. *J. Chem. Soc., Chem. Commun.* **1993**, 553. (c) Hamilton, B.; Rimmer, J. S.; Anderson, M.; Leigh, D. *Adv. Mater.* **1993**, *5*, 583.
(14) Rachdi, F.; Haijji, L.; Goze, C.; Jones, D. J.; Maireles-Torres, P.; Rozière, J. *Solid State Commun.* **1996**, *100*, 237.
(15) Masuhara, A.; Fujitsuka, M.; Ito, O. *Bull. Chem. Soc. Jpn.* **2000**, *73*, 2199.
(16) Paci, B.; Amoretti, G.; Arduini, G.; Ruani, G.; Shinkai, S.; Suzuki, T.; Ugozzoli, F.; Caciuffo, R. *Phys. Rev. B* **1997**, *55*, 5566.
(17) (a) de Brabander-van der Berg, E. M. M.; Meijer, E. W. *Angew. Chem., Int. Ed. Engl.* **1993**, *32*, 1308. (b) Jansen, J. F. G. A.; de Brabander-van der Berg, E. M. M.; Meijer, E. W. *Science* **1994**, *266*, 1226.
(18) Márquez, F.; Sabater, M. J. *J. Am. Chem. Soc.*, submitted for publication.
(19) *Introduction to Zeolite Science and Practice*; van Bekkum, H., Flanigen, E. M., Jansen, J. C., Eds.; Elsevier: Amsterdam, 1991.
(20) Thomas, J. K. *Acc. Chem. Res.* **1988**, *21*, 275.
(21) (a) Kresge, C. T.; Leonowicz, M. E.; Roth; W. J.; Vartuli; J. C.; Beck, J. S. *Nature* **1992**, *359*, 710. (b) Monnier, A.; Shutch, F.; Hou, Q. *Science* **1993**, *261*, 1299. (c) Beck, J. S.; Vartuli, J. C.; Roth, W. J. *J. Am. Chem. Soc.* **1992**, *114*, 834.
(22) Lobo, R.; Tsapatsis, M.; Freyhardt, C. C.; Khodabandeh, S.; Wagner, P.; Chen, C. Y.; Balkus, K. J.; Zones, S. I.; Davis, M. E. *J. Am. Chem. Soc.* **1997**, *119*, 8474, and references therein.
(23) *Light Scattering in Solids VIII*; Menendez, J., Page, J. B., Cardona, M., Guntherodt, G., Eds.; Springer: Berlin, 2000.
(24) Wang, S. Y.; Shen, W. Z.; Shen, X. C. *Appl. Phys. Lett.* **1995**, *67*, 783.
(25) Reber, C.; Yee, L.; Mckier, J.; Williams, R. S.; Tong, W. M.; Ohlberg, D. A.; Nan, R. L.; Zink, J. I.; Diederich, F. *J. Phys. Chem.* **1991**, *95*, 2127.
(26) Matus, M.; Kuzmany, H.; Sohmen, E. *Phys. Rev. Lett.* **1992**, *68*, 2822.
(27) Wang, Y. *J. Phys. Chem.* **1992**, *96*, 764.
(28) (a) Gu, G.; Ding, W.; Du, Y.; Huang, H.; Yang, S. *Appl. Phys. Lett.* **1997**, *70*, 2619. (b) Govindaraj, A.; Nath, M.; Eswaramoorthy, M. *Chem. Phys. Lett.* **2000**, *317*, 35.
(29) (a) Márquez, F.; Zicovich-Wilson, C. M.; Corma, A.; Palomares, E.; García, H. *J. Phys. Chem.* **2001**, *105*, 9973. (b) Márquez, F.; García, H.; Palomares, E.; Corma, A. Fernandez, L. *J. Am. Chem. Soc.* **2000**, *122*, 6520. (c) Márquez, F.; Martí, V.; Palomares, E.; García, H.; Adam, W. *J. Am. Chem. Soc.* **2002**, *124*, 7264.